

Pressure dependence of the superconducting critical temperature of $\text{HgBa}_2\text{Ca}_2\text{Cu}_3\text{O}_{8+y}$ and $\text{HgBa}_2\text{Ca}_3\text{Cu}_4\text{O}_{10+y}$ up to 30 GPa

D. Tristan Jover, R. J. Wijngaarden, H. Wilhelm, and R. Griessen

Department of Physics and Astronomy, Free University, De Boelelaan 1081, 1081 HV Amsterdam, The Netherlands

S. M. Loureiro and J.-J. Capponi

Laboratoire de Crystallographie, CNRS, Boîte Postale 166, 38042 Grenoble, France

A. Schilling and H. R. Ott

Laboratorium für Festkörperphysik, Eidgenössische Technische Hochschule Hönggerberg, 8093 Zürich, Switzerland

(Received 14 July 1995; revised manuscript received 20 November 1995)

By performing experiments on samples as pure as presently available, the origin of the reported pressure-induced T_c values well above 150 K in the mercury-based high- T_c superconductors has been investigated. For $\text{HgBa}_2\text{Ca}_2\text{Cu}_3\text{O}_{8+y}$ (Hg-1223) maximum T_c values between 142 K and 146 K are obtained under pressure up to 30 GPa, while for $\text{HgBa}_2\text{Ca}_3\text{Cu}_4\text{O}_{10+y}$ (Hg-1234) T_c never exceeds 121 K. To verify the reproducibility between different laboratories the pressure dependence of a sample from the same batch as the sample on which Nuñez-Regueiro reported a T_c value of 157 K at 23.5 GPa has also been measured. Below 10 GPa the agreement with his results is rather good and a possible explanation for the disagreement above 10 GPa is given. It appears that the reported high T_c values in non-single-phase Hg-1223 samples are due to the presence of Hg-1234 phase impurities. Also some of the adopted definitions of T_c have led to somewhat optimistic values of T_c : The high-pressure results on Hg-1223 found in the literature are therefore reviewed and reanalyzed. [S0163-1829(96)05830-4]

I. INTRODUCTION

The highest values for any superconducting transition temperature T_c have been observed in $\text{HgBa}_2\text{Ca}_2\text{Cu}_3\text{O}_{8+y}$ (Hg-1223) samples under very high pressures.¹⁻⁶ Even at ambient pressure Hg-1223, which was discovered by Schilling *et al.*,⁷ has set a new record value with a T_c as high as 134 K. Gao *et al.*⁸ performed the first high-pressure experiment on a Hg-1223 sample with at ambient pressure a T_c of 135 K. Under hydrostatic conditions they measured the superconducting transition resistively under pressure up to 1.7 GPa. They observed an increase in T_c up to 138 K at a rate of 1.8 K/GPa. These results are in very good agreement with those obtained by Klehe *et al.*⁹ Using a BeCu high-pressure cell they applied under purely hydrostatic conditions a pressure of 0.9 GPa on a Hg-1223 sample with at ambient pressure a T_c of 134 K. Determining T_c from ac-susceptibility measurements they observed an increase in T_c at a rate of 1.7 K/GPa. In a subsequent experiment Gao *et al.*^{2,3} were able to raise T_c above 150 K by applying a pressure of 18 GPa under quasihydrostatic conditions. Applying still higher pressures^{2,3} they even observed in one particular case superconductivity above 160 K at 31 GPa. Independently, Nuñez-Regueiro *et al.*⁴ observed superconductivity above 150 K at 23.5 GPa. Also Takahashi *et al.*⁵ were able to increase T_c above 150 K by applying pressure, although in their case this high T_c value was already reached at 11 GPa. It is very important at this point to determine whether the Hg-1223 phase really is responsible for the observed high T_c values and not a different superconducting minority phase (impurity phase) which could be present. In an attempt to do this Ihara

*et al.*⁶ measured the pressure dependence of a sample with a single superconducting Hg-1223 phase and two other samples containing also the superconducting $\text{HgBa}_2\text{Ca}_3\text{Cu}_4\text{O}_{10+y}$ (Hg-1234) phase. Surprisingly, the single-phase Hg-1223 sample reached a maximum T_c of only 140 K at 13 GPa, while the mixed-phase samples reached T_c 's of 150 K and 156 K at 25 GPa. From these results Ihara *et al.*⁶ concluded that the high T_c values in the mixed-phase samples are due to the presence of small amounts of Hg-1234 and that under pressure Hg-1234 should have a much higher T_c than Hg-1223. The main purpose of the present paper is to check whether the T_c of *pure* Hg-1234 can be raised above 150 K by performing similar measurements on Hg-1234 samples which are as pure as presently available.

In fact high-pressure measurements on Hg-1223 and Hg-1234 samples are interesting for two other reasons. From the schematic crystal structure of Hg-1223 and Hg-1234 shown in Figs. 1(a) and 1(b) it is obvious that the CuO_2 layers which are held responsible for superconductivity are not all identical since they have different surroundings. Therefore, both Hg-1223 and Hg-1234 have distinct inner (*i*) and outer (*o*) CuO_2 layers, contrary to high- T_c compounds with only one ($n=1$) or two ($n=2$) CuO_2 layers per unit cell. While the copper atoms of the inner CuO_2 layer(s) have a fourfold oxygen coordination, the copper atoms of the outer CuO_2 layers have a fivefold coordination. As a result the charge carrier density n_h and hence the intrinsic T_c may be different for the inner and outer CuO_2 layers.

The other reason for interest in these compounds is the relation between the maximum T_c at any pressure and the

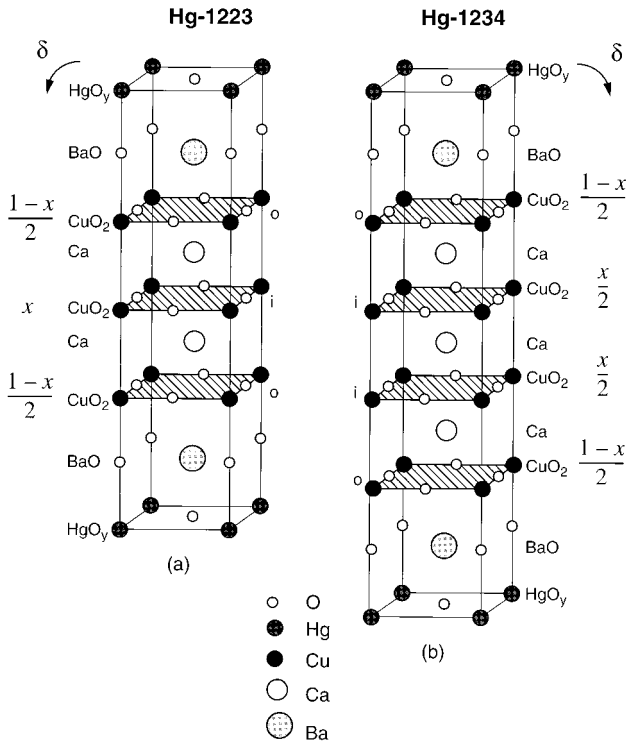


FIG. 1. Idealized structures of (a) $\text{HgBa}_2\text{Ca}_2\text{Cu}_3\text{O}_{8+y}$ (Hg-1223) and (b) $\text{HgBa}_2\text{Ca}_3\text{Cu}_4\text{O}_{10+y}$ (Hg-1234) with, respectively, three ($n=3$) and four ($n=4$) CuO_2 layers per unit cell. Both structures have *inequivalent* inner (*i*) and outer (*o*) CuO_2 layers. While the copper atoms of the inner CuO_2 layer(s) have a fourfold oxygen coordination, the copper atoms of the outer CuO_2 layers have a fivefold oxygen coordination.

number of CuO_2 layers per repeat unit. The general formula for the homologous series of the mercury-based high- T_c superconductors is given by $\text{HgBa}_2\text{Ca}_{n-1}\text{Cu}_n\text{O}_{2n+2+y}$ where n is the number of CuO_2 layers per unit cell. While some phenomenological models^{10–12} predict a monotonic increase of the maximum T_c for $n=1$ up to $n=4$, in the related $\text{Bi}_2\text{Sr}_2\text{Ca}_{n-1}\text{Cu}_n\text{O}_{2n+4+y}$ and $\text{Tl}_2\text{Ba}_2\text{Ca}_{n-1}\text{Cu}_n\text{O}_{2n+4+y}$ series the maximum T_c was experimentally found to occur in the $n=3$ compound under ambient conditions,^{13–15} but also under pressure.¹⁶ At ambient pressure the T_c of Hg-1223 is higher than that of Hg-1234. This could in principle be due to nonoptimal doping of the Hg-1234 compound. Since pressure generally increases the hole concentration, thereby increasing doping, it is interesting to verify whether the maximum T_c under pressure in the mercury-based compounds occurs for $n=3$ or for $n=4$. Attempts to vary the doping level in Hg-1223 via substitution of mercury by lead and oxygen anneals indicated¹⁷ that the maximum T_c at optimal doping in this compound is approximately 134 K.

This paper is organized as follows. In Sec. II two relevant phenomenological models are considered: In the first model a homogeneous charge distribution among all the CuO_2 layers within a unit cell is assumed while in the second model the possibility of an inhomogeneous distribution is explicitly taken into account. After a description of the sample preparation and the experimental details in Secs. III and IV, high-pressure results on several *high-purity* Hg-1223 and Hg-1234 samples are presented and discussed in Sec. V. These results

are then compared with existing data found in the literature. In order to do this it is necessary to briefly consider the various definitions of T_c and to use the same definition when comparing the results. Finally, a possible scenario for the apparent discrepancy between the various high-pressure experiments and the origin of the reported T_c values well above 150 K is given.

II. PHENOMENOLOGICAL MODELS

Since there is no microscopic theory for high- T_c superconductivity, two simple phenomenological models are discussed in this section in order to indicate which parameters could play an important role in reaching higher T_c 's. Other approaches are possible, but these are the most simple ones that contain the necessary elements. The discussion of these models is based on the crystal structures shown in Fig. 1, although it generally applies to other layered structures as well. In the first model¹⁸ it is assumed that the charge carriers or holes are distributed equally between all the CuO_2 layers within a unit cell regardless of their number, while in the second model¹⁹ the possibility of a nonhomogeneous charge distribution among the *inequivalent* CuO_2 layers in the $n=3$ and 4 compounds is explicitly taken into account.

In the *first* model, that of Wheatley *et al.*,¹⁸ T_c is mainly determined by the coupling between the CuO_2 layers. All the CuO_2 layers within a unit cell are taken to be equivalent, resulting in a homogeneous charge distribution, and only the coupling between nearest-neighbor CuO_2 layers is considered. The coupling between nearest-neighbor CuO_2 layers within a unit cell is Λ_i , while the coupling between the adjacent outer CuO_2 layers of neighboring unit cells is Λ_o . Both coupling parameters Λ_i and Λ_o are related to the interlayer transfer integrals $t_{\perp i}$ and $t_{\perp o}$, respectively, and to the intralayer exchange coupling parameter^{20–23} $J=4t_{\parallel}^2/U$ as follows:

$$\Lambda_{i,o} = \frac{t_{\perp i,o}^2}{J} = \frac{t_{\perp i,o}^2}{4t_{\parallel}^2} U, \quad (1)$$

where t_{\parallel} is the intralayer transfer integral and U is the on-site Coulomb repulsion.

For layered structures with one ($n=1$) CuO_2 layer per unit cell Wheatley *et al.*¹⁸ give the following relation for T_c :

$$T_c(1) = 2\Lambda_o c n_h, \quad (2)$$

where c is a constant of order unity and n_h is the hole doping with respect to half-filling, defined as the number of holes per CuO_2 layer and copper atom. At half-filling each copper site is occupied by a single electron which leads to insulating behavior. Adding holes results in an insulator-metal transition and superconductivity is experimentally observed for²⁴ $0.05 < n_h < 0.27$. Since Hg-1201 has a maximum T_c of 98 K at optimal doping,^{25,26} substituting this value for $T_c(1)$ in Eq. (2) yields $\Lambda_o c n_h = 49$ K.

For layered structures with two ($n=2$) CuO_2 layers per unit cell the following relation for T_c is found:¹⁸

$$T_c(2) = (\Lambda_o + \Lambda_i) c n_h. \quad (3)$$

Since Hg-1212 has a maximum T_c of 127 K at optimal doping,^{9,25} substituting this value for $T_c(2)$ (and for $\Lambda_o c n_h$ the previously found value of 49 K) yields $\Lambda_i c n_h = 78$ K. Assuming that neither c nor n_h change with the number n of CuO_2 layers per unit cell²⁷ implies that Λ_i is larger than Λ_o . This is consistent with the interlayer spacings.

For layered structures with three ($n=3$) and four ($n=4$) CuO_2 layers per unit cell the eigenvalue equations given by Wheatley *et al.*¹⁸ have to be solved. This leads to the following relations for T_c :

$$T_c(3) = \frac{1}{2} (\Lambda_o + \sqrt{\Lambda_o^2 + 8\Lambda_i^2}) c n_h \quad (4)$$

and

$$T_c(4) = \frac{1}{2} (\Lambda_o + \Lambda_i + \sqrt{\Lambda_o^2 + 5\Lambda_i^2 - 2\Lambda_o\Lambda_i}) c n_h. \quad (5)$$

Substituting in Eqs. (4) and (5) the values previously found for $\Lambda_o c n_h$ and $\Lambda_i c n_h$ yields $T_c(3) = 137$ K for the $n=3$ compound and $T_c(4) = 143$ K for the $n=4$ compound. The fact that ambient pressure experiments on the mercury-based high- T_c superconductors show that the maximum T_c is reached in the $n=3$ compound²⁸ implies that either Λ_i decreases or that optimal doping is never reached in the $n=4$ compound (conceivably because the charge reservoir layer does not contain enough holes to optimally dope all the CuO_2 layers). Under pressure it is expected that T_c increases since both Λ_o and Λ_i increase as the interlayer distances decrease.

In the *second* model, that of Haines and Tallon,¹⁹ the possibility of a nonhomogeneous charge distribution among the *inequivalent* CuO_2 layers in structures with three ($n=3$) or four ($n=4$) CuO_2 layers per unit cell is explicitly taken into account. Their model is based upon the assumption that each CuO_2 layer behaves as a superconducting structural unit with a well-defined intrinsic T_c which depends on the charge carrier density n_h of the layer under consideration. In the simplest case, T_c as a function of n_h follows the inverted parabolic dependence^{29,30}

$$T_c = T_{c\max} [1 - \beta(n_h - n_{h\max})^2], \quad (6)$$

with²⁹ $\beta = 82.6$ and $n_{h\max} = 0.16$. Even though the values of these parameters were obtained for $\text{La}_{2-z}\text{Sr}_z\text{CuO}_4$ it has been shown by Shafer and Penney²⁴ that they describe also the behavior of other high- T_c superconductors. The pressure dependence of n_h for most high- T_c superconductors³¹ lies in the range $dn_h/dp = 0.001 - 0.04$ holes per copper atom per GPa. More specifically for Hg-1223, from a local-density-approximation (LDA) electronic structure calculation Singh and Pickett³² find a value of $dn_h/dp = 0.002$ holes per copper atom per GPa for Hg-1223. For an increase in pressure by 20 GPa (hence $\Delta n_h = 0.04$), a change $\Delta T_c \approx 16$ K is calculated from Eq. (6) for a sample with initially $T_c = T_{c\max} = 120$ K, taking the parameter values mentioned above. For $T_c \neq T_{c\max}$, the change would be even larger. Clearly, from this calculation the pressure-induced change in n_h has a significant effect on T_c for Hg-1223; for Hg-1234 a similar behavior is expected. Although in principle the parameters $T_{c\max}$, β , and $n_{h\max}$ may also change under pres-

sure, for the present discussion the exact shape of T_c as a function of n_h is not essential and for simplicity will be referred to in the rest of this paper as an inverted parabola.

The charge distribution among the inequivalent CuO_2 layers is determined by minimizing the sum of band and Madelung energies as described below in more detail. Assuming that a *fraction* x of the total number δ of holes transferred from the charge reservoir (the charge reservoir being in this case the HgO_y layer) resides on the inner CuO_2 layer(s), a *fraction* $1-x$ has to reside on the outer CuO_2 layers (see Fig. 1). In this purely ionic model the total energy U_{tot} per unit cell is defined as the sum of a band energy U_b and the Madelung energy U_{Mad} :

$$U_{\text{tot}} = U_b + U_{\text{Mad}}. \quad (7)$$

Since in this model the holes are noninteracting, the band energy U_b for a particular CuO_2 layer is given by

$$U_b = \frac{\pi\hbar^2}{2m^*a^2} n_h^2, \quad (8)$$

where

$$n_h = \frac{x}{n-2} \delta \equiv n_h^{\text{inner}} \text{ for the inner } \text{CuO}_2 \text{ layer(s)} \quad (9a)$$

and

$$n_h = \frac{1-x}{2} \delta \equiv n_h^{\text{outer}} \text{ for the outer } \text{CuO}_2 \text{ layers,} \quad (9b)$$

since there are by definition two outer CuO_2 layers and $n-2$ inner CuO_2 layers in a compound with more than two CuO_2 layers per unit cell. In Eq. (8), m^* is the effective mass of holes in a parabolic CuO_2 band while a is the lattice parameter of the *square* CuO_2 layer. The total band energy is then the sum of contributions of all the CuO_2 layers within a unit cell. For the $n=3$ and 4 structures the following expressions are obtained:

$$U_b(x) = \frac{\pi\hbar^2}{2m^*a^2} \delta^2 \left(\frac{3x^2}{2} - x + \frac{1}{2} \right) \text{ for } n=3 \quad (10a)$$

and

$$U_b(x) = \frac{\pi\hbar^2}{2m^*a^2} \delta^2 \left(x^2 - x + \frac{1}{2} \right) \text{ for } n=4. \quad (10b)$$

Obviously, the total band energy alone leads to a homogeneous charge distribution since the minimum occurs at $x=1/3$ for $n=3$ and at $x=1/2$ for $n=4$. It is therefore the Madelung energy which is responsible for nonhomogeneous charge distributions. As shown by Haines and Tallon¹⁹ the Madelung energy can be written as a function of δ and x :

$$U_{\text{Mad}} = \frac{e^2 \delta}{2\epsilon S} [b_0 + b_1 \delta + (b_2 + b_3 \delta)x + b_4 \delta x^2], \quad (11)$$

where e is the electron charge, ϵ is the dielectric constant introduced here to take into account all the charge carriers which are not included in the parabolic CuO_2 bands, and S is the average Wigner-Seitz radius. The coefficients b_i only depend on the distribution of holes between the copper and

oxygen sites within the CuO_2 layers and the crystal structure. Both U_b and U_{Mad} and hence U_{tot} are therefore a function of x . The charge distribution among the inequivalent CuO_2 layers is now found by minimizing U_{tot} with respect to x . As a result

$$x_{\min} = \frac{1 - A_p(b_2/\delta + b_3)}{3 + 2A_p b_4} \quad \text{for } n=3 \quad (12a)$$

and

$$x_{\min} = \frac{1 - A_p(b_2/\delta + b_3)}{2(1 + A_p b_4)} \quad \text{for } n=4, \quad (12b)$$

where A_p is defined as

$$A_p = \frac{e^2}{\hbar^2} \frac{a^2}{\pi S} \frac{m^*}{\epsilon} \quad (13)$$

and x_{\min} is the value of x for which U_{tot} is a minimum. The charge carrier density of the inner and outer CuO_2 layers in Hg-1223 and Hg-1234 is therefore not the same. Assuming that δ increases with pressure, the charge distribution between the inequivalent CuO_2 layers also changes as a function of pressure. In passing note that the first model mentioned could easily be adapted in order to take also the inequivalence of the CuO_2 layers in compounds with $n > 2$ into account.

III. SAMPLE PREPARATION AND CHARACTERIZATION

In this work the superconducting transition of several Hg-1223 and Hg-1234 samples from Zürich (Z) and Grenoble (G) has been measured resistively under very high pressure. The Hg-1223 sample from Zürich will be denoted in the rest of this paper by Hg-1223 Z while the Hg-1223 samples from Grenoble will be denoted by Hg-1223 G1 and Hg-1223 G2, respectively. In a similar way the Hg-1234 samples from Grenoble will be identified as Hg-1234 G1 and Hg-1234 G2.

The sample Hg-1223 Z (containing 60% of Hg-1223 but no other superconducting phase) was prepared following the procedure described by Putilin *et al.*³³ From a well-ground mixture of the respective nitrates $\text{Ba}(\text{NO}_3)_2$, $\text{Ca}(\text{NO}_3)_2$, and $\text{Cu}(\text{NO}_3)_2$, sintered at 900 °C, a precursor material with nominal composition $\text{Ba}_2\text{CaCu}_2\text{O}_{5+y}$ was first prepared. After successively regrinding and mixing with powdered HgO, pellets were pressed from the so obtained mixture. These pellets were then sealed in evacuated quartz tubes, placed in steel containers and held at 800 °C for 5 h. After cooling down to room temperature the pellet from which the sample Hg-1223 Z is obtained was annealed at 300 °C in flowing oxygen for several hours.

The samples Hg-1223 G1 and Hg-1223 G2 (both samples containing more than 95% of Hg-1223), as well as the samples Hg-1234 G1 (containing more than 80% of Hg-1234) and Hg-1234 G2 (containing more than 90% of Hg-1234), were prepared under high pressure in a belt-type apparatus of the Laboratoire de Crystallographie and at high temperatures. As described by Antipov *et al.*,³⁴ a precursor material with nominal composition $\text{Ba}_2\text{Ca}_2\text{Cu}_3\text{O}_{7+y}$ was prepared in a similar way as described above by mixing the respective nitrates in appropriate amounts. The mixture thus

obtained was initially heated at 600 °C in air for 12 h, and then reground and annealed at 925 °C in flowing oxygen for 72 h with three intermediate regrindings. Powdered HgO was added and the reactant mixture thoroughly grounded and successively sealed in a gold capsule. Samples with predominantly the Hg-1223 phase or the Hg-1234 phase were obtained by carrying out the reactions at a pressure of 1.8 GPa and at an annealing temperature of 920 °C for 1.6, 1.6, 3.5, and 1.7 h, respectively. The samples Hg-1223 Z, Hg-1223 G1, and Hg-1223 G2 were optimally doped with an ambient T_c around 134 K, while the samples Hg-1234 G1 and Hg-1234 G2 were slightly underdoped with an ambient T_c around 115 K. For an underdoped sample the highest T_c under pressure is expected since in such a sample T_c increases both due to an increase in charge carrier concentration³¹ and due to intrinsic effects.^{9,30,35–38}

IV. EXPERIMENTAL DETAILS

Using a cryogenic diamond anvil cell³⁹ (DAC), made entirely of stainless steel, pressure is generated and applied to the samples. Its principle of operation is based on pushing two parallel aligned diamonds towards each other using a lever-based system. In this work 16-sided diamond anvils are used with a culet (high-pressure face) diameter of typically 0.85 mm. In order to reduce pressure gradients across the edges of the culet, the diamonds are single beveled under an angle of 5°. The diameter of the culet and bevel together is typically 1.2 mm. Under these conditions resistive measurements up to pressures as high as 30 GPa are possible within this DAC.

In order to support the diamond anvils and to sustain the quasi-hydrostatic pressures generated in the DAC a 100 μm thick stainless steel foil, known as the gasket, is used. In the center of the gasket a hole with a diameter of 300 μm is drilled which serves as sample space. This space is then completely filled with sample material. In this case the sample itself acts as its own pressure transmitting medium. Depending upon the sample, the pressure medium may influence the T_c vs p behavior as shown by Klotz and Schilling.⁴⁰ However, while Klotz and Schilling⁴⁰ found a marked change in the T_c vs p behavior of a $\text{Bi}_2\text{Sr}_2\text{CaCu}_2\text{O}_{8+y}$ (Bi-2212) single crystal using a pressure medium and no pressure medium at all, a study by van Eenige⁴¹ shows that the use of a pressure transmitting medium does not influence the measurement noticeably if the sample is polycrystalline. For example, experiments on $\text{YBa}_2\text{Cu}_4\text{O}_8$ (Y-124) under quasi-hydrostatic conditions⁴² and similar experiments under hydrostatic conditions⁴³ gave practically the same results for T_c vs p . Since the mechanical properties of Hg-1223 and Hg-1234 lie intermediate between those of Bi-2212 and Y-124, the use of a pressure medium is expected to have some influence, but not a drastic one. Besides the sample material, several very small ruby chips are also included in the sample space to allow a direct determination of the applied pressure, also as a function of position on the sample. At 30 GPa, the pressure gradient $\Delta p/p$ is at most 20% between the center of the sample and its edge. The area between the contacts for resistivity measurements experiences a gradient of less than 10%. The piece of ruby closest to the center of this area was used for the pressure determination.

Pressure can be changed at any temperature simply by turning a knob at the top of the cryostat. The applied pressure is determined *in situ*, close to the superconducting transition of the samples, with the ruby fluorescence method. After correction for the temperature-induced shift of the ruby R_1 fluorescence line⁴⁴ the calibration of Mao *et al.*⁴⁵ is used. For the excitation of the ruby an Ar⁺-ion laser is operated at 514.5 nm. The fluorescence spectrum of ruby is then detected with an optical multichannel analyzer (OMA).

The advantages of the ruby fluorescence method to determine the applied pressure are manifold. For the purpose of this paper it is important to note that it allows measuring pressure *in situ* at any temperature as long as the position of the ruby R_1 line is corrected for temperature. This is an important improvement over the lead (Pb) manometer method used by several other groups^{1,2,4,6} where the pressure has to be determined at the superconducting transition temperature of Pb, close to liquid helium temperatures. It is also an improvement over the method where the pressure is determined from the pressure-induced phase transitions in bismuth at room temperature.¹ Since the T_c values of the Hg-1223 and Hg-1234 samples are much higher than the T_c value of Pb and considerably below room temperature, and since pressure may change significantly when changing the temperature in most high-pressure generating apparatuses, this may lead to serious errors in determining the applied pressure.

The temperature of the sample is measured using a standard platinum resistor placed in a copper block in which one of the diamonds is mounted. Since at low temperatures diamond has an even higher thermal conductivity than copper, there is a good thermal contact between sample and thermometer. To check for possible thermal gradients in the body of the high-pressure cell two other platinum resistors are mounted approximately 1 cm above and below the diamond anvils. The temperature difference is found to be 0.6 K. Interpolated linearly, this corresponds to a temperature difference across the sample of 3 mK.

The sample can be cooled by flowing liquid helium through a heat exchanger at the bottom of the DAC while its temperature can be increased by passing a current through a constantan wire heater, wound around the high-pressure cell. In this way the temperature of the sample can be varied continuously between 10 K and 300 K under control of a temperature regulator.

The superconducting transition temperature T_c of the sample is determined resistively using the standard four-probe technique. For this purpose only four electrical leads to the sample are strictly needed. In practice six leads are placed on top of one of the diamonds in order to have two spare ones. These leads consist of flattened gold wires with a diameter of 25 μm which are pressed onto the sample for electrical contact. Since the gasket is placed on top of the gold wires, it has to be insulated. This is done by gluing a thin kapton foil to the gasket using a 1:1 mixture of Al_2O_3 powder with an average grain size of 0.05 μm and epoxy adhesive. The four-point resistance $R(T)$ of the sample as a function of temperature is then measured with a Keithley 2001 multimeter using a current of 1 mA.

V. EXPERIMENTAL RESULTS AND DISCUSSION

In Figs. 2 and 3 typical superconducting transitions of the Hg-1223 and Hg-1234 samples are shown at different pressures. Under pressure the polycrystalline samples break up into smaller grains. Since the intergrain boundaries are not superconducting, they are responsible for residual resistances observed at temperatures below T_c . After subtraction of these residual resistances at 100 K for the Hg-1223 samples and at 90 K for the Hg-1234 samples, the superconducting transitions are normalized with respect to their values at 160 K and 140 K, respectively. The values of the residual resistances RR and the normal-state resistances R_n for Hg-1223 and Hg-1234 are given in Table I. Under pressure the normal-state resistance above T_c often changes from a metallic to a semiconducting behavior. In two samples (Hg-1223 G1 and Hg-1223 G2) this semiconducting behavior is most clear around 10 GPa and disappears at much higher pressures. This behavior is usually ascribed to properties of the intergrain boundaries and is therefore not related to superconductivity at all. The changing background fortunately has only a very limited effect upon the determination of T_c . Even when under pressure some broadening occurs, the superconducting transition remains clearly visible and well defined.

However, it is clear that due to broadening of the transition under pressure different definitions of T_c may lead to significantly different values of T_c . In fact, the apparent discrepancy between the T_c vs p results published so far by various high-pressure groups can be partially attributed to different definitions of T_c . Some of these definitions are shown in Fig. 4. T_{ct} is defined as the intersection of the tangent through the inflection point of the resistive transition with a straight-line fit of the normal state just above the transition. T_{cd} is obtained from the first derivative $\partial R/\partial T$ of the resistive transition with respect to temperature. It is defined as the intersection of the tangent through the point where $\partial^2 R/\partial T^2$ has the largest negative value with the extrapolation of the normal-state behavior just above the transition. T_{cv} is defined as the temperature where $\partial R/\partial T$ starts to deviate from the approximately constant high-temperature behavior.

Before proceeding with a discussion about the various high-pressure results of other high-pressure groups, the results obtained in this work for T_{ct} and T_{cd} will be presented now. While T_{ct} is less sensitive to paraconductivity and hence might be closer to the thermodynamic T_c , T_{cd} is useful for comparison with the results published so far. T_{cv} can obviously not be identified with the true critical temperature T_c since it is related to the onset of superconducting fluctuations which may be considerable above T_c in these high- T_c layered compounds. The anisotropy of the mercury-based compounds lies intermediate between those of $\text{YBa}_2\text{Cu}_3\text{O}_7$ (Y-123) and the very anisotropic bismuth-based compounds.⁴⁶

In Fig. 5, T_{ct} and T_{cd} are shown as a function of pressure for the three different Hg-1223 samples studied in this work. All the samples exhibit a relatively large increase of T_c up to approximately 10 GPa. At higher pressures T_{ct} clearly continues to increase for Hg-1223 Z, saturates for Hg-1223 G1, and decreases slightly for Hg-1223 G2. This last sample is of

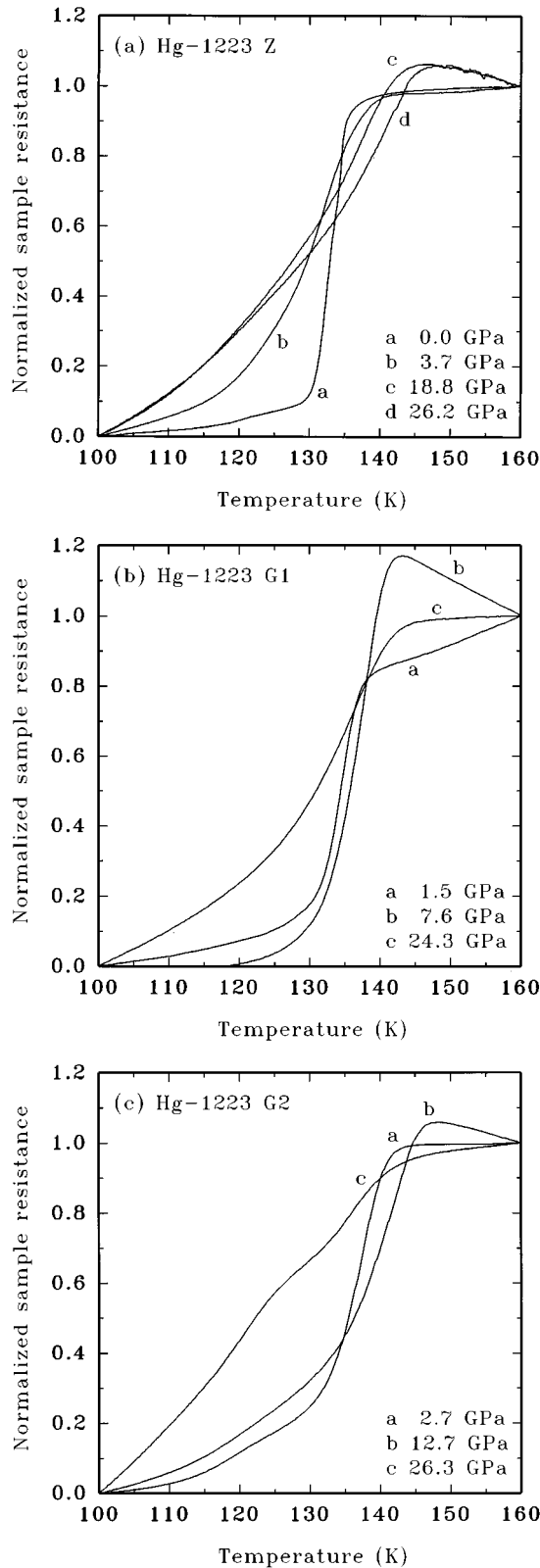


FIG. 2. Superconducting transitions of (a) Hg-1223 Z, (b) Hg-1223 G1, and (c) Hg-1223 G2 at different pressures. After subtraction of the residual resistance at 100 K the superconducting transitions are normalized with respect to their values at 160 K. Under pressure the normal-state behavior in Hg-1223 G1 and Hg-1223 G2 changes from metallic to semiconducting and back to metallic.

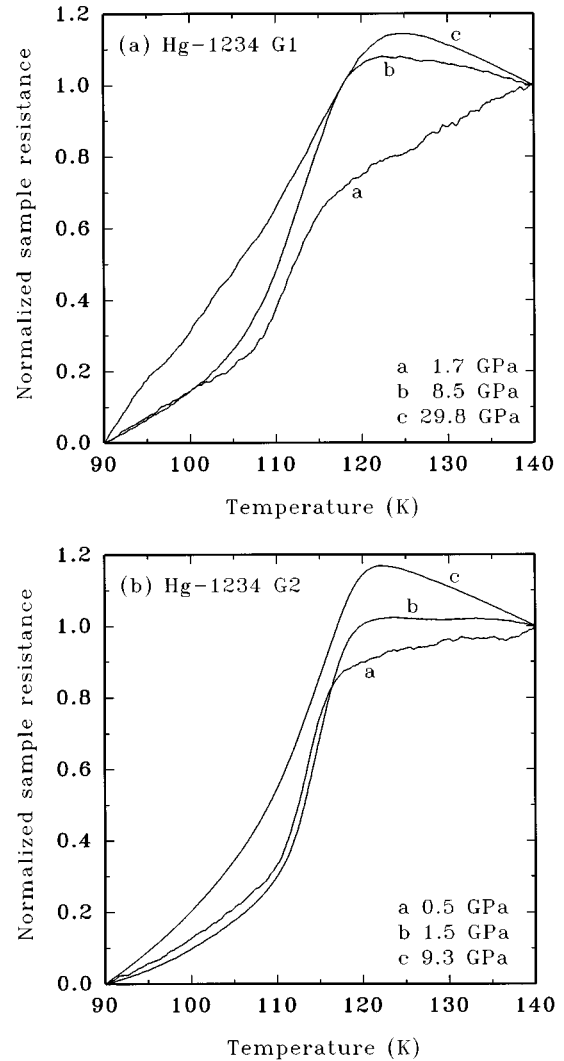


FIG. 3. Superconducting transitions of (a) Hg-1234 G1 and (b) Hg-1234 G2 at different pressures. After subtraction of the residual resistance at 90 K the superconducting transitions are normalized with respect to their values at 140 K. Under pressure the normal-state behavior in Hg-1234 G1 and Hg-1234 G2 changes from metallic to semiconducting.

the same batch as the sample measured by Nuñez-Regueiro *et al.*⁴ Their results are also included in Fig. 5(c). Since they used T_{cv} as a definition of T_c , their published results have been reanalyzed in terms of T_{cd} to allow a meaningful comparison. Although at low pressures there is a good agreement, at pressures above 10 GPa the behavior is quite different. A possible explanation is that the oxygen concentration is not the same in both samples. During preparation of ceramic samples of typically 1 cm^3 a gradient in the oxygen concentration may develop. Hence, the small grains of typically 10^{-5} cm^3 used in high-pressure experiments can differ in oxygen concentration, even when taken from the same batch.

In Fig. 6 most of the high-pressure results published so far on Hg-1223 samples are shown together with the results obtained in this work. Where necessary the results have been reanalyzed in terms of T_{cd} , again to allow a meaningful comparison. In their original publication, Nuñez-Regueiro *et al.*⁴ used T_{cv} which is approximately 3 K higher than T_{cd} .

TABLE I. Residual resistances RR at 100 K for Hg-1223 and 90 K for Hg-1234 and normal-state resistances R_n at 160 K for Hg-1223 and 140 K for Hg-1234 for the superconducting transitions shown in Figs. 2 and 3.

Sample	p (GPa)	RR (Ω)	R_n (Ω)
Hg-1223 Z	0.0	4.3	22.8
	3.7	23.9	54.3
	18.8	15.1	24.7
	26.2	12.5	19.7
Hg-1223 G1	1.5	1.9	4.3
	7.6	0.95	1.5
	24.3	2.5	3.1
Hg-1223 G2	2.7	2.3	5.2
	12.7	1.1	2.2
	26.3	0.3	0.4
Hg-1234 G1	1.7	1.0	2.2
	8.5	0.6	0.9
	29.8	10.3	13.4
Hg-1234 G2	0.5	15.4	23.9
	1.5	3.1	4.6
	9.3	2.6	4.2

For the discussion of the new high-pressure results on Hg-1223 presented in this paper, now the T_{cd} values shown in Fig. 5 are used. The results shown in Fig. 6 can roughly be divided into two groups: group (a) where T_c does not exceed 148 K and group (b) where T_c reaches values well above 150

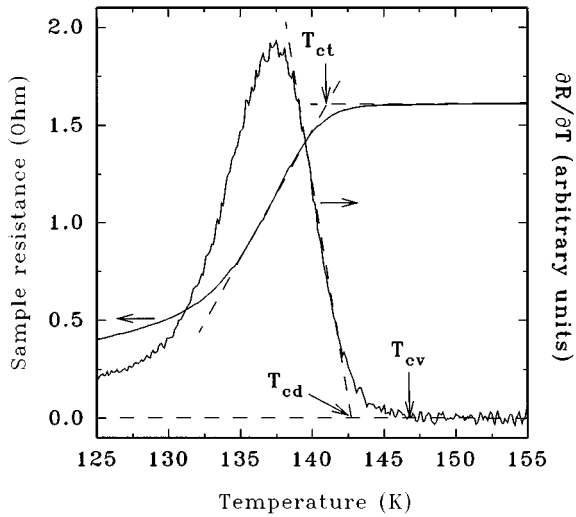


FIG. 4. Plot of the resistive transition $R(T)$ of Hg-1223 G2 as a function of temperature and its first derivative $\partial R/\partial T$ with respect to temperature at 2.7 GPa. This plot is used to illustrate the various definitions of T_c used in the literature. T_{ct} is defined as the intersection of the tangent through the inflection point of the resistive transition with a straight-line fit of the normal state just above the transition. T_{cd} is defined as the intersection of the tangent through $\partial R/\partial T$ where $\partial^2 R/\partial T^2$ has the largest negative value with the extrapolation of the normal-state behavior just above T_c . T_{cv} is defined as the temperature where $\partial R/\partial T$ starts to deviate from the approximately constant high-temperature behavior.

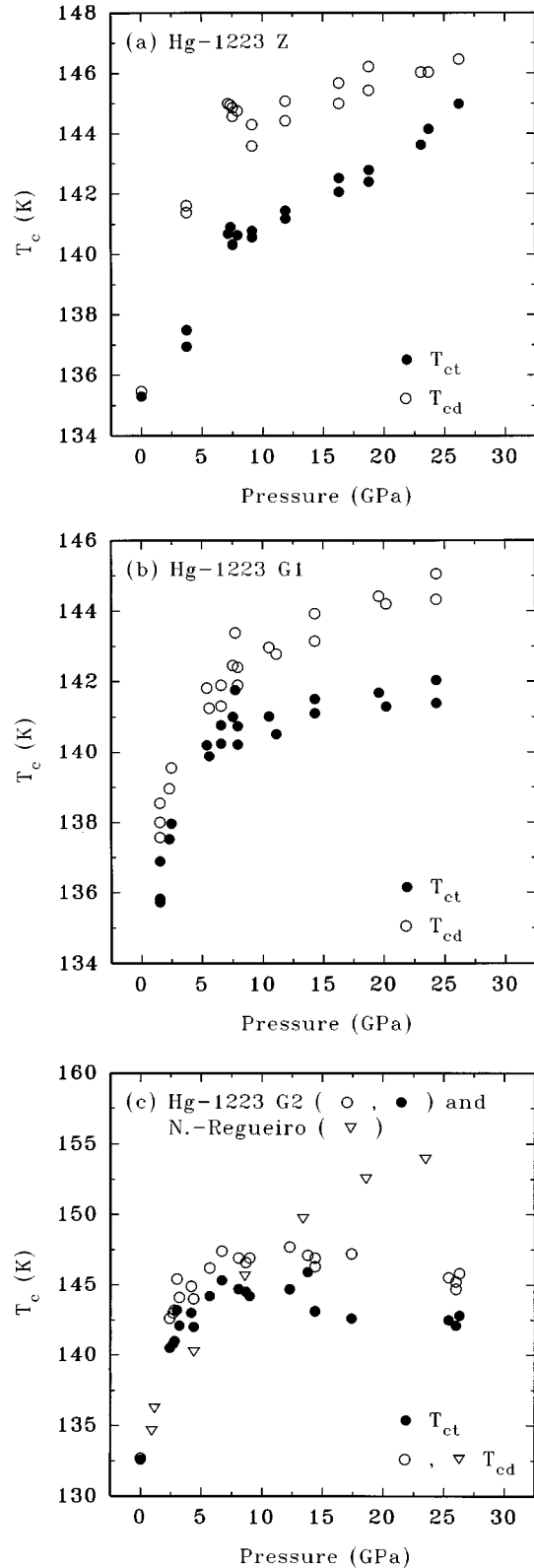


FIG. 5. Pressure dependence of the superconducting transition temperatures T_{ct} and T_{cd} of (a) Hg-1223 Z, (b) Hg-1223 G1, and (c) Hg-1223 G2 up to 26 GPa. In (c) the high-pressure results of Nuñez-Regueiro *et al.* (Ref. 4) are also included. Below 10 GPa the agreement with the results obtained in this work is rather good. For the definition of T_{ct} and T_{cd} see Fig. 4.

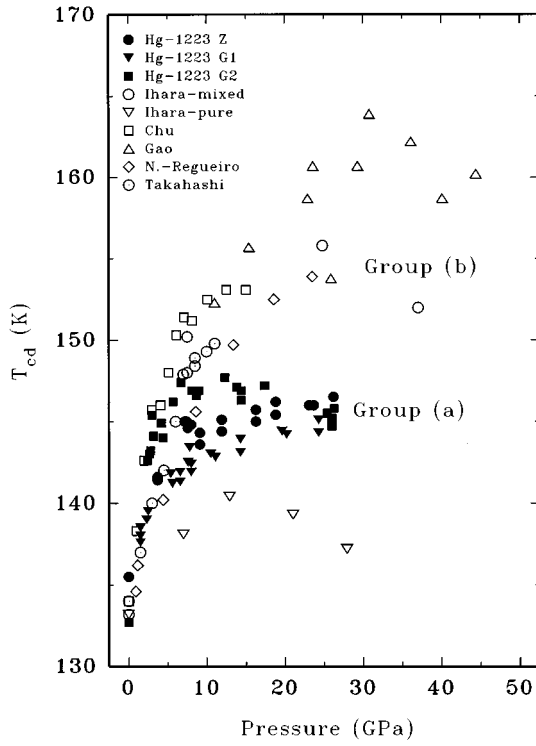


FIG. 6. Pressure dependence of the superconducting transition temperature T_{cd} of Hg-1223 obtained in this work (solid symbols) and from the literature (open symbols). For the definition of T_{cd} see Fig. 4. The results published by Nuñez-Regueiro *et al.* (Ref. 4) were reanalyzed in terms of T_{cd} . The remaining results are from the following references: Chu *et al.* (Ref. 1) Gao *et al.* (Refs. 2,3), Takahashi *et al.* (Ref. 5) and Ihara *et al.* (Ref. 6). The large spread at high pressures is possibly due to a different oxygen concentration of the samples. These results can roughly be divided into two groups labeled group (a) and group (b).

K. Apart from the high-pressure results of Nuñez-Regueiro *et al.*,⁴ group (b) includes the results of Chu *et al.*,¹ Gao *et al.*,^{2,3} and the results of Ihara *et al.*⁶ on one of the mixed-phase Hg-1223 samples. Considering the results of Ihara *et al.*⁶ the high T_c values of group (b) could be explained, as they pointed out, by the hypothesis that under pressure Hg-1234 has a higher T_c than Hg-1223 and that hence the superconducting Hg-1234 minority phase can short-circuit the rest of the sample. In order to verify whether the T_c of Hg-1234 is indeed higher than that of Hg-1223, the pressure dependence of *high-purity* Hg-1234 has been measured. The result is shown in Fig. 7. At ambient pressure the T_c of Hg-1234 is considerably lower than that of Hg-1223. From resistive measurements a T_c of 114–116 K (extrapolated values from the T_c vs p curves) is found, while from ac-susceptibility measurements an average value of 115 K is obtained. Also under pressure the T_c of the Hg-1234 samples remain lower than that of the Hg-1223 samples, in contradiction with the hypothesis that under pressure Hg-1234 should have a higher T_c than Hg-1223. Clearly, this conclusion is based on the high-purity Hg-1234 samples measured in this work. However, the possibility that the Hg-1234 minority phase in the experiment of Ihara *et al.*⁶ is of a different composition or (being embedded in Hg-1223) experiencing a different strain cannot be ruled out.

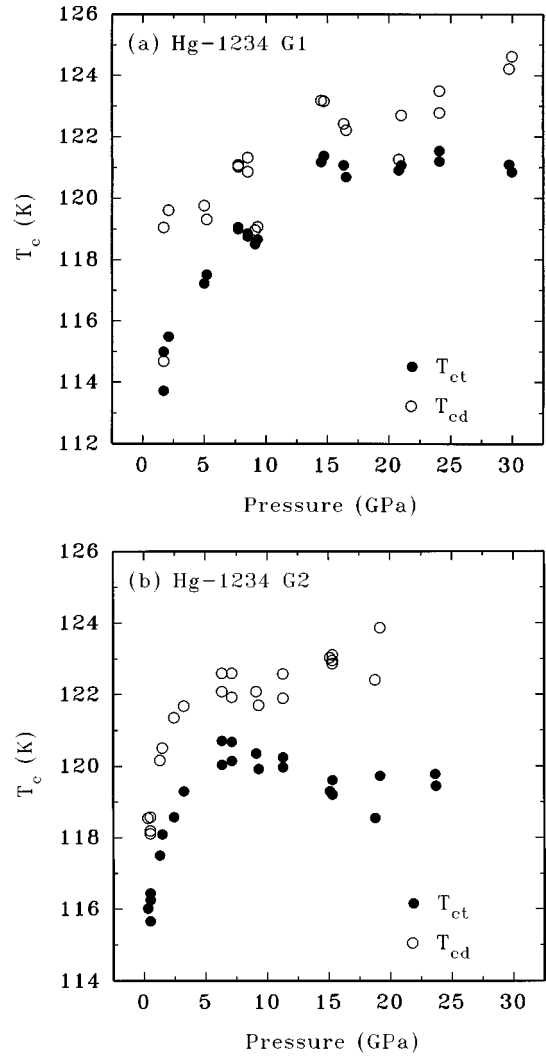


FIG. 7. Pressure dependence of the superconducting transition temperature T_{ct} and T_{cd} of (a) Hg-1234 G1 and (b) Hg-1234 G2 up to 30 GPa. For the definition of T_{ct} and T_{cd} see Fig. 4.

While comparison of all these results is difficult due to possibly different pressure conditions, the results presented in this paper have all been obtained under the same conditions, enabling a fair comparison. Now the different behavior of T_c vs p in the Hg-1223 samples will be discussed in terms of the model of Haines and Tallon¹⁹ described in Sec. II. In this model the inequivalence of the inner and outer CuO_2 layers is explicitly taken into account. The total amount of doping δ of all the CuO_2 layers is partially due to oxygen off-stoichiometry and partially due to pressure-induced doping, i.e., $\delta = \delta_y + \delta_p$. Using the model of Haines and Tallon¹⁹ the distribution of δ among the CuO_2 layers is then found and hence also the charge carrier density n_h^{inner} of the inner CuO_2 layer(s) and n_h^{outer} of the outer CuO_2 layers. Considering a layered structure with three CuO_2 layers per unit cell Fig. 8(a) shows as an example a possible charge distribution satisfying the condition $n_h^{\text{inner}} + 2n_h^{\text{outer}} = \delta$. Even though both n_h^{inner} and n_h^{outer} increase linearly with δ , the rate at which they do so is not the same. The intrinsic T_c of each CuO_2 layer follows now directly from the parabolic behavior shown in Fig. 8(b) and the charge carrier density n_h of that

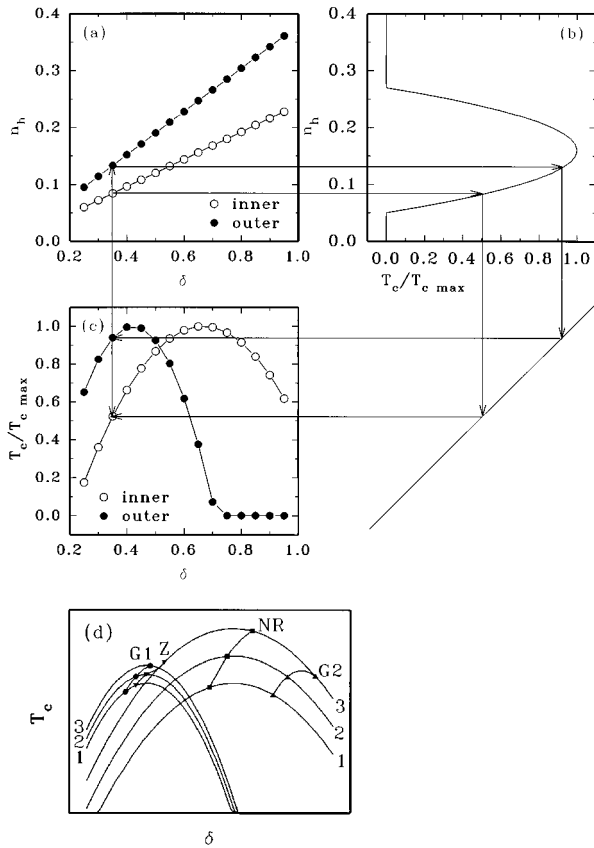


FIG. 8. (a) Possible charge distribution among the inner and outer CuO₂ layers in a layered structure with three CuO₂ layers per unit cell. The charge carrier density n_h^{inner} on the inner CuO₂ layer and n_h^{outer} on the outer CuO₂ layers has to satisfy the condition $n_h^{\text{inner}} + 2n_h^{\text{outer}} = \delta$. (b) Parabolic dependence of T_c upon the charge carrier concentration n_h needed to calculate (c) the intrinsic T_c 's of the inequivalent CuO₂ layers as a function of δ . (d) Possible explanation of the experimental results obtained in this work assuming that $T_{c\max}$ also depends on pressure.

layer. Since in Fig. 8(a) n_h^{inner} and n_h^{outer} are given as a function of δ , a relation for the intrinsic T_c as a function of δ can be calculated for the inner and outer CuO₂ layers, respectively. The result is a different parabolic function of T_c vs δ for each kind of layer [see Fig. 8(c)]. If δ_p increases linearly with pressure,³¹ then $\delta = \delta_y + \alpha p$ which implies that the horizontal axis in Fig. 8(c) can be replaced by a pressure axis. The starting point at ambient pressure depends upon the actual value of δ_y .

Under pressure the total doping δ of the sample increases and the T_c of the sample as a whole will therefore follow from the two parabolas. The resultant T_c will either be the maximum of the two curves (in absence of proximity coupling) or intermediate between the two curves (in presence of proximity coupling). In any case a complicated behavior as a function of pressure is expected. This behavior can be even more complicated, as depicted in Fig. 8(d), if the fact is taken into account³⁵ that in general also $T_{c\max}$ increases with pressure. The experimental results obtained in this work will now be interpreted in terms of the model just described. In absence of proximity coupling, the T_c of the sample as a whole follows the highest intrinsic T_c of the superconducting

CuO₂ layers. In Fig. 8(d) the parabolas labeled “1” correspond to ambient pressure. If $T_{c\max}$ increases as a function of pressure,³⁵ and if this increase is larger for the inner CuO₂ layer, at higher pressures the parabolas labeled “2” and at still higher pressures the parabolas labeled “3” are obtained. The various experimental curves can now easily be reproduced if at ambient pressure different values for δ_y and hence different starting points are taken. The schematic curves shown in Fig. 8(d) are labeled according to the corresponding experimental curves, where NR is used to represent all the high-pressure results in group (b) of Fig. 6. From calculations performed by Haines and Tallon¹⁹ it appears that at low pressures the T_c of the sample Hg-1223 Z is determined by the inner CuO₂ layer. Above 14 GPa the total (ambient pressure plus pressure-induced) doping of the sample has shifted to a point where T_c is determined by the outer CuO₂ layers. Because of this, the T_c of Hg-1223 Z starts to increase again above 14 GPa. At ambient pressure Hg-1223 G1 is at the left-hand side of the left-hand parabola and even up to 25 GPa the doping cannot be increased enough to follow the right-hand parabola. As already mentioned in Sec. II, a saturation of T_c at higher pressures could also mean that simply no charge carriers are available any more in the charge reservoir layer. The sample Hg-1223 G2 is on the right-hand side of the right-hand parabola, and after an initial increase due to the increase of $T_{c\max}$ with pressure, the down-going slope dominates and T_c decreases. The curve NR is at the most favorable position: T_c increases both due to the increase of $T_{c\max}$ and due to the shape of the parabola.

It is assumed here that $T_{c\max}$ increases at a faster rate for the curves NR and G2 than for the other curves. This can be due either to a larger $\partial T_{c\max}/\partial p$ for the outer CuO₂ layers or to an enhanced T_c due to the presence of Hg-1234 phase impurities. Such an enhancement of T_c by a secondary phase has previously been observed by Raffy *et al.*⁴⁷ in BiSrCaCuO superlattices. They report that the T_c of multilayers consisting of ultrathin Bi-2212 layers separated by metallic Bi-2201 layers is enhanced remarkably with respect to single phase Bi-2212 films prepared under the same conditions. Unfortunately the results of this high-pressure experiment cannot discriminate between these two interpretations.

For Hg-1234 a comparison with the literature is not possible due to the lack of other high-pressure experiments on Hg-1234. The pressure dependence of the two Hg-1234 samples in Fig. 7 can be understood in a similar way as discussed for Hg-1223 since Hg-1234 G1 behaves very much like Hg-1223 G1 and Hg-1234 G2 like Hg-1223 G2.

At this point it must be emphasized that the scenario discussed above yields a possible but not a necessary explanation of the observed behavior in the mercury-based high- T_c compounds Hg-1223 and Hg-1234 under pressure.⁴⁸ The experiments on the Hg-1234 samples show clearly that the Hg-1234 phase investigated in the present experiment cannot be responsible for the pressure-induced enhancement of T_c in multiphase materials to values well above 150 K. On the other hand, it cannot be ruled out that another Hg-1234 phase (e.g., differently doped; a similar case for Y-123 is discussed in Ref. 36) is responsible. Another possibility is that the Hg-1223 and Hg-1234 phases alternate on an atomic scale in the mixed-phase samples. Then it is not inconceivable that both the doping levels and internal strains are significantly

different from the pure compounds, which in principle could result in higher T_c values.

VI. CONCLUSION

Using a cryogenic diamond anvil cell the pressure dependence of the superconducting critical temperature of Hg-1223 and Hg-1234 has been measured resistively under quasihydrostatic conditions up to 30 GPa. At ambient pressure, these compounds with, respectively, three ($n=3$) and four ($n=4$) CuO_2 layers per unit cell have T_c 's of 133–135 K and 114–116 K. The results of several high-pressure experiments on different samples of Hg-1223 and Hg-1234 show that at low pressures T_c increases relatively fast, while at higher pressures T_c may either increase further, saturate, or even decrease, depending on the particular sample. This behavior can be explained in terms of a model involving *inequivalent* CuO_2 layers. From the high-pressure results presented in this paper it appears that neither *pure* Hg-1223 nor *pure* Hg-1234 on its own is responsible for the observed T_c values above 145 K. Samples containing both supercon-

ducting phases, on the other hand, have reached much higher values of T_c .

ACKNOWLEDGMENTS

One of the authors (D.T.J.) would like to thank Dr. E. M. Haines for a very pleasant collaboration and illuminating discussions during her stay in Amsterdam and Dr. J. L. Tallon for his support and his interest in high-pressure experiments. H.W. acknowledges the *Human Capital and Mobility Program* of the European Community under Contract No. ERB-CHBICT 940952 for its financial support and the hospitality of the Free University in Amsterdam. The efforts of Dr. D. G. de Groot have been useful for the interpretation of the results presented in this paper. This work is part of the research program of the Stichting voor Fundamenteel Onderzoek der Materie (FOM) which is financially supported by NWO. The work in Zürich was in part financially supported by the Schweizerische Nationalfonds zur Förderung der Wissenschaftlichen Forschung.

-
- ¹C. W. Chu, L. Gao, F. Chen, Z. J. Huang, R. L. Meng, and Y. Y. Xue, *Nature (London)* **365**, 323 (1993).
- ²L. Gao, Y. Y. Xue, F. Chen, Q. Xiong, R. L. Meng, D. Ramirez, C. W. Chu, J. H. Eggert, and H. K. Mao, *Phys. Rev. B* **50**, 4260 (1994).
- ³L. Gao, Y. Y. Xue, F. Chen, Q. Xiong, R. L. Meng, D. Ramirez, C.W. Chu, J. H. Eggert, and H. K. Mao, *Physica C* **235-240**, 1493 (1994).
- ⁴M. Nuñez-Regueiro, J.-L. Tholence, E. V. Antipov, J.-J. Capponi, and M. Marezio, *Science* **262**, 97 (1993).
- ⁵H. Takahashi, A. Tokiwa-Yamamoto, N. Môri, S. Adachi, H. Yamauchi, and S. Tanaka, *Physica C* **218**, 1 (1993).
- ⁶H. Ihara, M. Hirabayashi, H. Tanino, K. Tokiwa, H. Ozawa, Y. Akahama, and H. Kawamura, *Jpn. J. Appl. Phys.* **32**, L 1732 (1993).
- ⁷A. Schilling, M. Cantoni, J. D. Guo, and H. R. Ott, *Nature (London)* **363**, 56 (1993).
- ⁸L. Gao, Z. J. Huang, R. L. Meng, J. G. Lin, F. Chen, L. Beauvais, Y. Y. Sun, Y. Y. Xue, and C. W. Chu, *Physica C* **213**, 261 (1993).
- ⁹A.-K. Klehe, J. S. Schilling, J. L. Wagner, and D. G. Hinks, *Physica C* **223**, 313 (1994).
- ¹⁰C.-H. Eab and I.-M. Tang, *Phys. Lett. A* **134**, 253 (1989).
- ¹¹J. L. Birman and J.-P. Lu, *Phys. Rev. B* **39**, 2238 (1989).
- ¹²C.-H. Eab and I.-M. Tang, *Phys. Rev. B* **40**, 4427 (1989).
- ¹³M. Kikuchi, S. Nakajima, Y. Syono, K. Hiraga, T. Oku, D. Shindo, N. Kobayashi, H. Iwasaki, and Y. Muto, *Physica C* **158**, 79 (1989).
- ¹⁴K. A. Müller, in *Highlights in Condensed Matter Physics and Future Prospects*, Vol. 285 of *NATO Advanced Study Institute, Series B: Physics*, edited by L. Esaki (Plenum Press, New York, 1991), p. 453.
- ¹⁵M. Di Stasio, K. A. Müller, and L. Pietronero, *Phys. Rev. Lett.* **64**, 2827 (1990).
- ¹⁶D. Tristan Jover, R. J. Wijngaarden, R. S. Liu, J. L. Tallon, and R. Griessen, *Physica C* **218**, 24 (1993).
- ¹⁷A. Schilling, M. Cantoni, O. Jeandupeux, J. D. Guo, and H. R. Ott, in *Proceedings of the 6th International Symposium on Superconductivity ISS 93*, edited by T. Fujita and Y. Shiohara (Springer-Verlag, Tokyo, 1994), p. 231.
- ¹⁸J. M. Wheatley, T. C. Hsu, and P. W. Anderson, *Nature (London)* **333**, 121 (1988).
- ¹⁹E. M. Haines and J. L. Tallon, *Phys. Rev. B* **45**, 3172 (1992).
- ²⁰C. L. Cleveland and R. Medina, *Am. J. Phys.* **44**, 44 (1976).
- ²¹G. Baskaran, Z. Zou, and P. W. Anderson, *Solid State Commun.* **63**, 973 (1987).
- ²²K. A. Chao, J. Spalek, and A. M. Oleś, *J. Phys. C.* **10**, L 271 (1977).
- ²³A. H. MacDonald, S. M. Girvin, and D. Yoshioka, *Phys. Rev. B* **37**, 9753 (1988).
- ²⁴M. W. Shafer and T. Penney, *Eur. J. Solid State Inorg. Chem.* **27**, 191 (1990).
- ²⁵S. M. Loureiro (private communication).
- ²⁶A.-K. Klehe, A. K. Gangopadhyay, J. Diederichs, and J. S. Schilling, *Physica C* **213**, 266 (1992).
- ²⁷For a large number n of CuO_2 layers per unit cell, however, the charge carrier density n_h of each layer may actually decrease with increasing n . For $n=2$ this effect is believed to be negligible.
- ²⁸B. A. Scott, E. Y. Suard, C. C. Tsuei, D. B. Mitzi, T. R. McGuire, B.-H. Chen, and D. Walker, *Physica C* **230**, 239 (1994).
- ²⁹J. L. Tallon and J. R. Cooper, in *Advances in Superconductivity V*, edited by Y. Bando and H. Yamauchi (Springer-Verlag, Tokyo, 1993), p. 339.
- ³⁰R. P. Gupta and M. Gupta, *Phys. Rev. B* **51**, 11 760 (1995).
- ³¹R. J. Wijngaarden, J. J. Scholtz, E. N. van Eenige, and R. Griessen, in *Frontiers of High Pressure Research*, Vol. 286 of *NATO Advanced Study Institute, Series B: Physics*, edited by H. D. Hochheimer and R. D. Ethers (Plenum Press, New York, 1992), p. 399, and references therein.
- ³²D. J. Singh and W. E. Pickett, *Physica C* **233**, 237 (1994).
- ³³S. N. Putilin, E. V. Antipov, O. Chmaissem, and M. Marezio, *Nature (London)* **362**, 226 (1993).

- ³⁴E. V. Antipov, S. M. Loureiro, C. Chaillout, J.-J. Capponi, P. Bordet, J.-L. Tholence, S. N. Putilin, and M. Mazzi, *Physica C* **215**, 1 (1993).
- ³⁵R. J. Wijngaarden, E. N. van Eenige, J. J. Scholtz, and R. Griessen, *Physica C* **185-189**, 787 (1991).
- ³⁶J. J. Neumeier and H. A. Zimmermann, *Phys. Rev. B* **47**, 8385 (1993).
- ³⁷J. J. Neumeier, *Physica C* **233**, 354 (1994).
- ³⁸C. C. Almasan, S. H. Han, B. W. Lee, L. M. Paulius, M. B. Maple, B. W. Veal, J. W. Downey, A. P. Paulikas, Z. Fisk, and J. E. Schirber, *Phys. Rev. Lett.* **69**, 680 (1992).
- ³⁹J. J. Scholtz, A. Driessen, R. van den Berg, H. van Groen, H. Verhoog, J. J. de Kleuver, R. J. Wijngaarden, and R. Griessen, *High Press. Res.* **5**, 874 (1990).
- ⁴⁰S. Klotz and J. S. Schilling, *Physica C* **209**, 499 (1993).
- ⁴¹E. N. van Eenige, Ph.D. thesis, Vrije Universiteit, Amsterdam, 1991.
- ⁴²J. J. Scholtz, E. N. van Eenige, R. J. Wijngaarden, and R. Griessen, *Phys. Rev. B* **45**, 3077 (1992).
- ⁴³D. Braithwaite, G. Chouteau, G. Martinez, J. L. Hodeau, M. Mazzi, J. Karpinski, E. Kaldis, S. Rusiecki, and E. Jilek, *Physica C* **178**, 75 (1991).
- ⁴⁴I. F. Silvera and R. J. Wijngaarden, *Rev. Sci. Instrum.* **56**, 121 (1985).
- ⁴⁵H. K. Mao, J. Xu, and P. M. Bell, *J. Geophys. Res.* **91**, 4673 (1986).
- ⁴⁶A. Schilling, O. Jeandupeux, J. D. Guo, and H. R. Ott, *Physica C* **216**, 6 (1993).
- ⁴⁷H. Raffy, S. Labdi, Z. Z. Li, H. Rifi, S. F. Kim, S. Megtert, O. Laborde, and P. Monceau, *Physica C* **235-240**, 182 (1994).
- ⁴⁸In fact the total doping δ (which is the sum of the doping n_h^{inner} of the inner CuO_2 layers and n_h^{outer} of the outer CuO_2 layers) increases as a function of pressure. In the model of Haines and Tallon (Ref. 19) either n_h^{inner} and n_h^{outer} both increase as a function of pressure or one increases while the other decreases (the total doping δ always increasing with pressure). In the text it is assumed for simplicity that both n_h^{inner} and n_h^{outer} increase with increasing δ . In the other situation a very similar argument can be made.